A Practical Low-Boom Overpressure Signature Based on Minimum Sonic Boom Theory

Robert J. Mack
NASA Langley Research Center
Hampton, VA

George T. Haglund
Boeing Commercial Airplane Company
Seattle, WA

SUMMARY

A brief resume of sonic boom minimization methods is given to provide a background for a new, empirical modification of the Seebass and George minimum-nose-shock sonic boom F-function and signature. The new "hybrid" F-function has all the inherent flexibility of application found with the Darden-modified Seebass and George F-function. In addition, it has enhanced this flexibility and applicability with neglegible increase in nose and/or tail shock strength. A description of this "hybrid" F-function and signature is provided, and the benefits of using them to design high-performance, low-boom aircraft are discussed.

INTRODUCTION

The theory of minimum sonic boom has advanced considerably since the L. B. Jones report on a lower bound to sonic boom, reference 1, in 1961. Based on the flow field of a supersonic projectile paper by G. B. Whitham, reference 2, Jones predicted that a slender body whose area growth was proportional to $x^{1/2}$ would produce a minimum disturbance overpressure signature in the far field.

Walkden, reference 3, showed that the lift on a wing-body also contributed to the far-field overpressure because, along the longitudinal or flight direction, it generated equivalent area which was directly proportional to the product of the local lift and the Mach number parameter, β, and was inversely proportional to the cruise velocity dynamic pressure. With this extension to Whitham's theory, the L. B. Jones lower bound body could now represent both the volume and the lift of the aircraft. However, the nose bluntness of the lower bound body meant that aircraft it represented would be subject to a sizeable zero-lift wave drag penalty.

While evaluating the overpressures generated by large aircraft during the acceleration to

cruise velocity, reference 4, F. E. McLean noted that equivalent-area body shapes with less wave drag than the Jones lower bound body produced lower intensity shocks at distances in the mid-field range. Studies of sonic boom propagation through a standard stratified atmosphere by W. D. Hayes, reference 5, demonstrated that the shape of the pressure signature would tend to stabilize or "freeze" while the shock strengths attenuated as the disturbances travelled the mid-field distances between the stratospheric cruise altitude and the ground. These studies changed the focus of minimization from the far-field to the mid-field.

The low boom and minimum boom signatures used today came from the mid-field studies of R. Seebass and A. R. George, reference 6, who applied minimization techniques to pressure signature shapes. They provided a means by which the overall aircraft design could be guided and controlled to reduce the shock strengths felt on the ground. These methods still led to aircraft with some low-boom-induced drag penalties although they were usually lower than previous levels found on the lower bound equivalent area body. However, with the modification to the nose-bluntness requirement introduced by C. M. Darden in reference 7, trade-offs between shock strength and aircraft drag could be conducted during the design phases that showed promise of providing aerodynamically efficient, mission-capable aircraft with acceptable sonic boom characteristics.

Another modification to the overpressure signature shape recently contributed by G. T. Haglund, reference 8, further opened the "window" of design flexibility for the aircraft designer integrating both low sonic boom and high aerodynamic efficiency characteristics into the aircraft configuration. Like the Darden nose-bluntness modification, it was suggested by a merging of experience with the Seebass and George minimum boom pressure signatures with purely practical design considerations. The purpose of this report is to show why and how this "second generation" sonic boom signature was developed and demonstrate the benefits derived from applying it to conceptual aircraft design methodology.

SYMBOLS

A_e	aircraft equivalent areas, ft^2
B	value of the F-function slope between $y = \xi$ and $y = l_e$, ft
C	value of the F-function between $y = y_f$ and $y = \xi$, ft
D	discontinuous change in the F-function at $y = \lambda$, ft
F(y)	the Whitham F-function
h	cruise altitude, ft
H	value of the F-function at $y = y_f / 2$
I(x)	unit step function; I(a) equals 1.0 only for $x \geq a$, it is zero elsewhere

K_r ground reflection factor, usually 1.9

l_e effective length of the aircraft or model, ft

M cruise Mach number

p flow field pressure, psf

p_a ambient pressure, psf

Δp $p - p_a$, psf

q free stream dynamic pressure, psf

W beginning cruise weight, lb

x longitudinal distance, ft

x_e effective distance, ft

y effective distance parameter in the F-function, F(y)

y_f F-function "nose-bluntness" parameter, ft

y_r effective distance along trailing F-function where tail shock conditions are met

α value of the atmospheric "advance factor", $\Delta F(y)/\Delta y$

α_x atmospheric advance defined in reference 6, $\alpha_x = C / \alpha$, ft

β $\sqrt{M^2 - 1.0}$

λ effective length that determines the shape of the positive portion the F-function, ft

ξ effective length where "ramp" of slope B begins, ft

ϕ angle whose tangent is equal to the value of B, see figure 7

DEVELOPMENT

L. B. Jones, one of the first to research minimum sonic boom body shapes, derived his lower bound body from impulse theory. It has rapid local area growth at the nose followed by smaller area growth such that the equivalent area distribution of this lower bound sonic boom body is proportional to $x^{1/2}$. With this F-function, an N-wave shaped far-field overpressure signature with the lowest ground overpressure level is obtained. However, the drag increment associated with the local nose bluntness can be prohibitively large. Figure 1 shows the equivalent area distribution, the F-function, and the pressure signature of a typical Jones lower bound body.

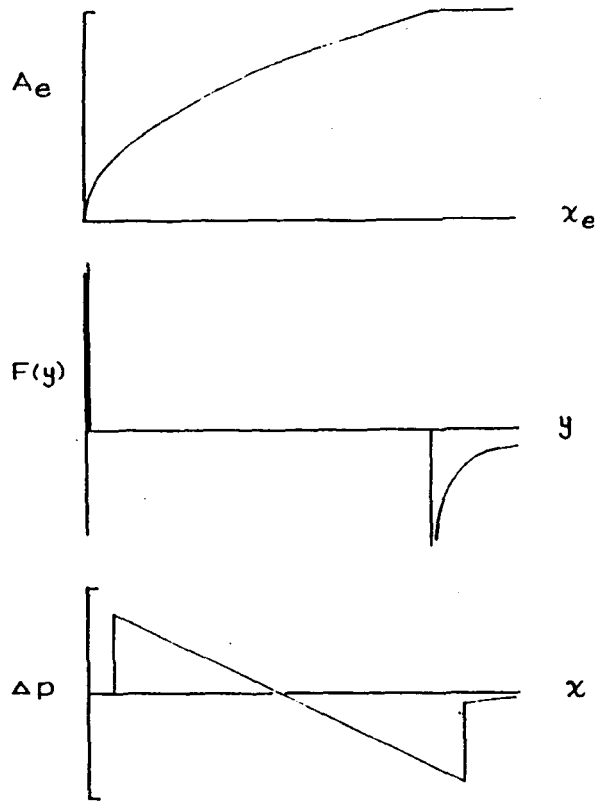

Figure 1. Area distribution, F-function, and pressure signature of a Jones lower bound body.

When later research and design studies indicated that supersonic-cruise aircraft would be long and slender enough so that the mid-field rather than the far-field signature would reach the ground, other types of body shapes were examined for both low boom and low wave drag characteristics. The minimization techniques used by Seebass and George provided two pressure signatures which were constrainted for either minimum nose shock or minimum peak overpressure. Both of these are shown in figure 2 as presented in their original form.

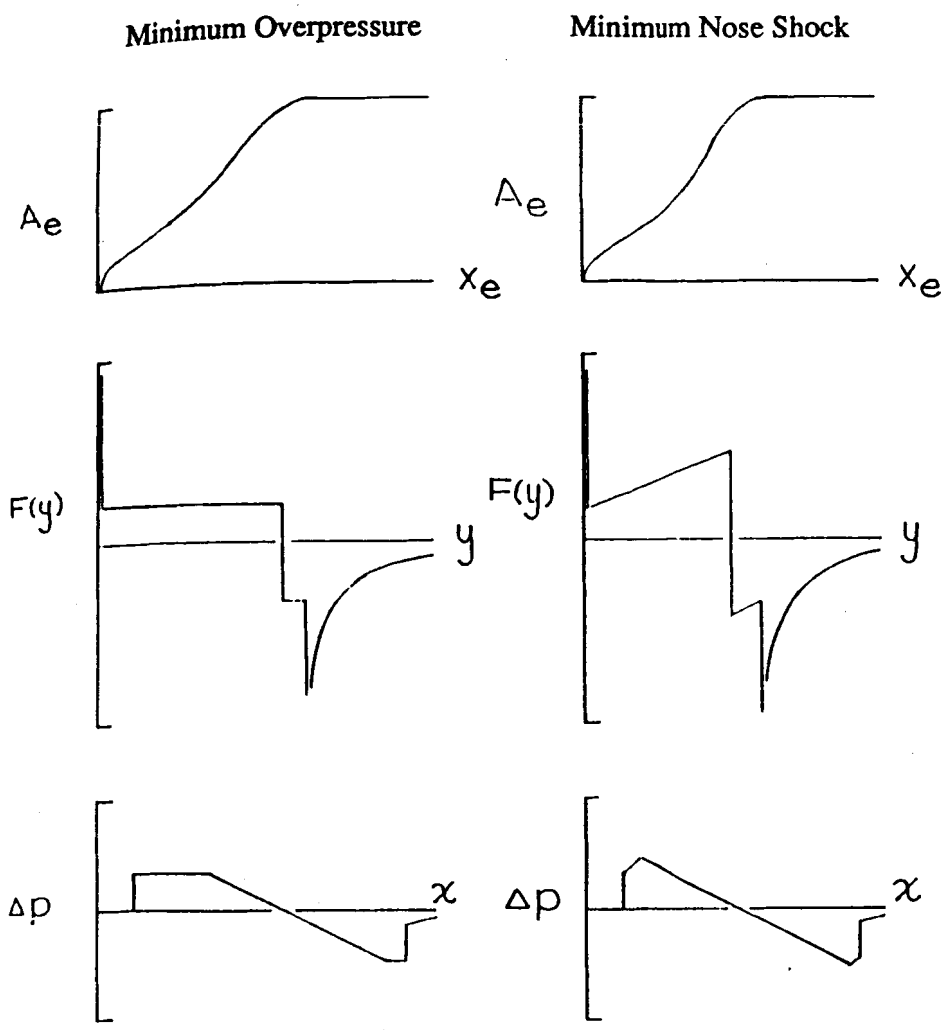

Figure 2. Seebass and George minimized pressure signatures, equivalent areas, and F-functions.

Note that both of these signatures come from F-functions with Dirac delta-functions at their origins, just like the Jones lower-bound-body F-function. They are different in that the distributed area behind the delta-function permits a lower nose shock solution for a specified cruise altitude than that provided by the Jones lower bound body for an aircraft of the same length and weight.

By replacing the Dirac delta function with a narrow adjustable nose "spike", as shown in figure 3 for the minimum overpressure signature F-function, the drag of the vehicle can be reduced at the cost of a small increase in shock strength.

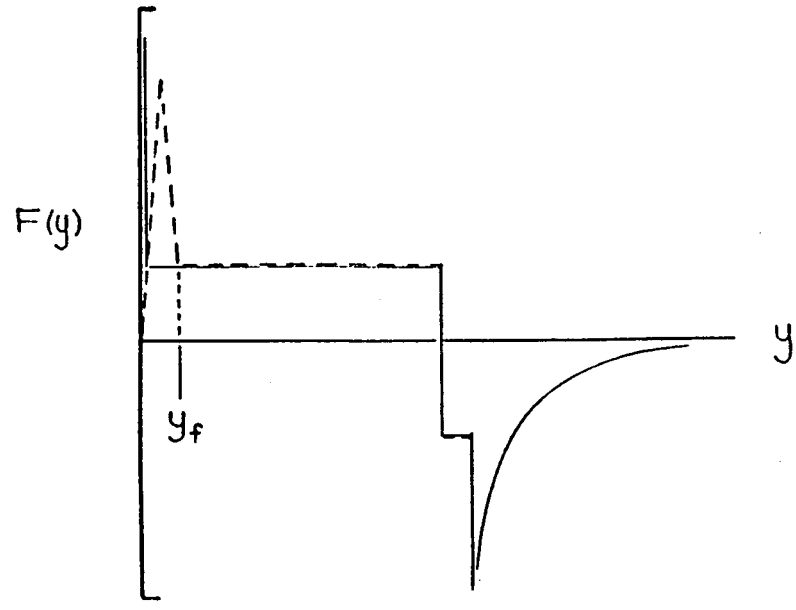

Figure 3. Nose "spike" modification to the "flat top" F-function.

With this modification, the configuration drag can be varied during the design stages. Trade-offs between drag and ground overpressure permit more flexibility in selecting and integrating aircraft components.

Although not shown, the modified Seebass and George minimum shock or "ramp" F-function, reference 6, can be obtained by the addition of a "spike". In addition to the nose "spike" width, y_f, the slope of the "ramp" length, B (see symbol list and figure 2), can also be adjusted to permit more component arrangement flexibility in the aircraft design.

Both of the minimum boom F-functions and signatures are point-design shapes with point-design limitations. The "flat-top" signature has one forward of the $y = y_f$ point on the F-function, while the "ramp" F-function and pressure signature has one on each side of the $y = y_f$ point. With the "ramp" F-function, perturbations to the ambient conditions of the standard atmosphere will change the atmospheric propagation characteristics resulting in higher overpressures. The "flat-top" F-function is somewhat less sensitive in that atmospheric perturbations in only one direction will produce higher overpressures.

These design point features indicate that the "ramp" and the "flat-top" signatures can be minimized only for a narrow range of atmospheric propagation characteristics. This poses no problem when designing research or wind tunnel models, but is a potential difficulty when designing a real supersonic cruise aircraft. Since the standard atmosphere is an averaged statistical

model, aircraft configurations designed with it and these two F-functions have limited value because only an average set of flight conditions are being considered and met.

G. Haglund made a further practical modification to the F-function and pressure signature to overcome these point-design limitations. Like the nose "spike" feature which preceded it, the modification was empirical and increased the applicability and flexibility of the low-boom methodology at the potential expense of a small increase in nose shock strength. The derivation of the equivalent areas from the F-function and a description of the F-function features are outlined in the following section.

In figure 4, this "second generation"-modified F-function, pressure signature, and equivalent area distribution are presented.

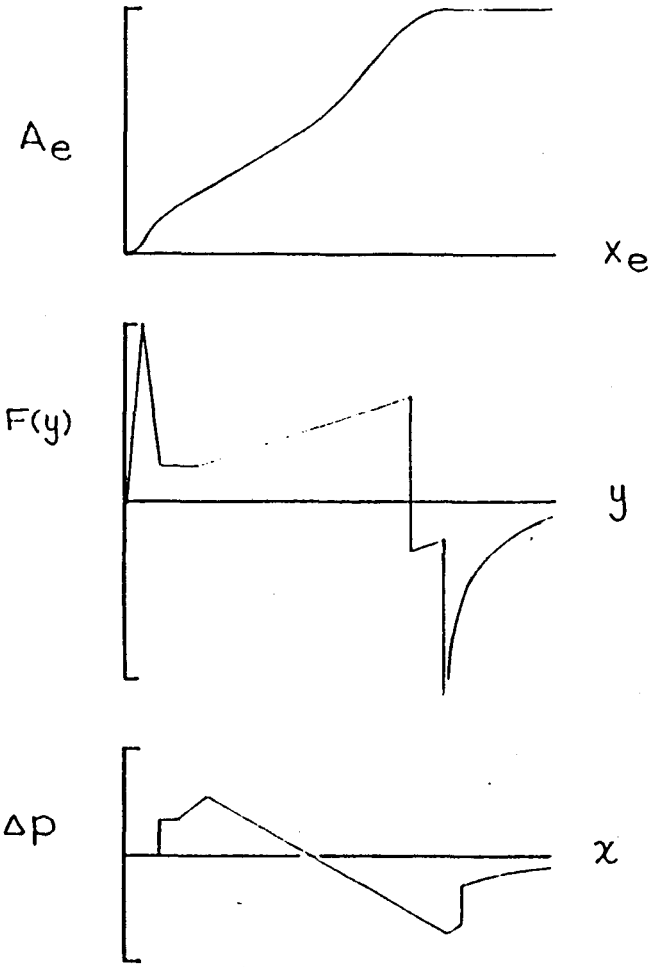

Figure 4. Haglund-modified equivalent areas, F-function, and pressure signature.

This F-function is no longer a true minimized F-function nor does it give a true minimized pressure signature in the classical mathematical definition. However, for practical aerodynamic and acoustic reasons, it combines the best features of the Seebass and George F-functions and the nose

"spike"(for drag- nose shock trades), with a constant-value section between the "spike" and the "ramp". Such an F-function and its derivative signature is more accurately called a "hybrid".

The constant-value section aft of y_f in the F-function permits hot-day and cold-day perturbations in the atmospheric propagation characteristics to be incorporated into the aircraft design as well as allowing additional control over aircraft length, component arrangement and integration, and area growth. With this feature on the F-function and its incorporation in the aircraft geometry, the probability that the ground shock strength would be predictable for a specified Mach number, altitude and beginning cruise weight could be greatly improved. The following paragraphs will describe these two features.

Atmospheric compensation. The method for incorporating hot-day, cold-day atmospheric propagation variations can be explained with the use of figure 5.

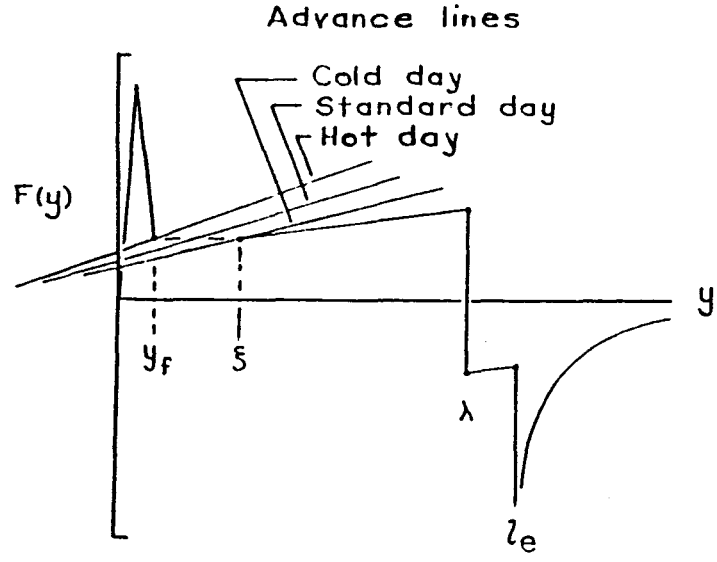

Figure 5. Hybrid F-function showing hot-day/ cold-day compensation analysis.

For given flight conditions of cruise Mach number, altitude, ground overpressure, and weight, the atmospheric propagation advance is computed for the standard day, the hot day, and the cold day. Cold-day conditions decrease the value of the atmospheric "advance factor" resulting in a "spike" length that is longer than one required for a standard day. Conversely, hot-day conditions increase the atmospheric "advance factor" value relative to that for a standard day and the "spike" length is shorter. This inverse relationship between the atmospheric "advance factor" and "spike" length is due to the definition of the "advance factor" which represents the net change in a finite-pressure signal location relative to a zero-strength acoustic signal traveling through the atmosphere.

The lower value of the advance factor could determine the location of the "nose bluntness" length, y_f, while the highest value of the advance could determine the most forward location of

the "ramp" starting point, ξ. With these two values in hand, the remaining signature parameters of Mach number, cruise altitude, aircraft effective length, slope of "ramp", and cruise weight would be input to the Hybrid Signature code. Computed values of Δp would be compared with desired overpressure limits. Adjustments to the input, excluding y_f and ξ, would be tried iteratively until a satisfactory F-function, equivalent area distribution, and signature was found with ξ no less that the value set by cold-day conditions.

Usually, the "spike" length, y_f, is varied to study the trade-off between shock strength and zero-lift wave drag. It still can be used for this purpose as long as the hot-day/cold-day atmospheric advance compensations are not compromised. There can still be length available for a larger value of ξ which would be useful in giving sufficient aircraft volume to meet mission requirements of fuel volume, passenger cabin room, reserve fuel, landing gear stowage, etc. Two examples are given to show the sensitivity of the method.

The first is for an aircraft which cruises at a Mach number of 3.0 :

$M = 3.0$,

$h = 73{,}000$ ft ,

$W = 650{,}000$ lb ,

$l_e = 300.0$ ft ,

$\xi = 40.0$ ft , and

$B = 0.5\ \alpha$

For a 1962 standard atmosphere day, the value $y_f = 20.0$ ft results in a $\Delta p = 1.032$ psf. To obtain the same value of Δp on a "hot day", y_f needs to be about 18.0 ft, while for a "cold day", y_f would be about 22.0 ft. So if an overpressure of 1.032 psf is an acceptable nose shock strength, then 18.0 feet value provides the necessary "cold day" compensation. The aircraft will have a bit more nose bluntness and probably a bit more drag than if it were designed for a standard day, but it will meet the desired nose shock criteria for all but the most extreme atmospheric conditions. The hot-day and the cold-day atmospheres were approximations to those defined in the 1962 standard atmosphere tables. However, the results obtained with their use indicated the probable values and the ranges in "hybrid" signature-calculation constants determined with more exact methods.

The second example is for an aircraft which cruises at a Mach number of 1.6 :

$M = 1.6$,

$h = 45{,}000$ ft ,

$W = 650{,}000$ lb ,

$l_e = 300.0$ ft ,

$\xi = 40.0$ ft , and

$B = 0.5\ \alpha$

For the standard day, $y_f = 20.0$ ft results in $\Delta p = 0.617$ psf. For the "hot day", y_f of about 19.0 ft is appropriate, while for the "cold day", y_f is about 21.0 ft. The plus-and-minus differential of "hot day" minus "cold day" y_f values are very small at either Mach number. Thus, only the "hot day" value is of primary importance. Most of the time, the value of ξ is greater than the yf value required for "cold day" compensation. This permits additional flexibility in adjusting the desired low boom equivalent areas for good agreement with those of the conceptual aircraft being designed.

The Δp value of 0.617 psf looks attractive but should not be taken seriously without further examination. In this example, the aircraft nose geometry which would produce such a ground nose shock strength was prohibitively slender. Thus, nose geometry as well as overpressure is a consideration in the selection of an equivalent area distribution.

Design flexibility. The advantages of using the Haglund "hybrid" F-function method during the preliminary design phases are illustrated in figure 6.

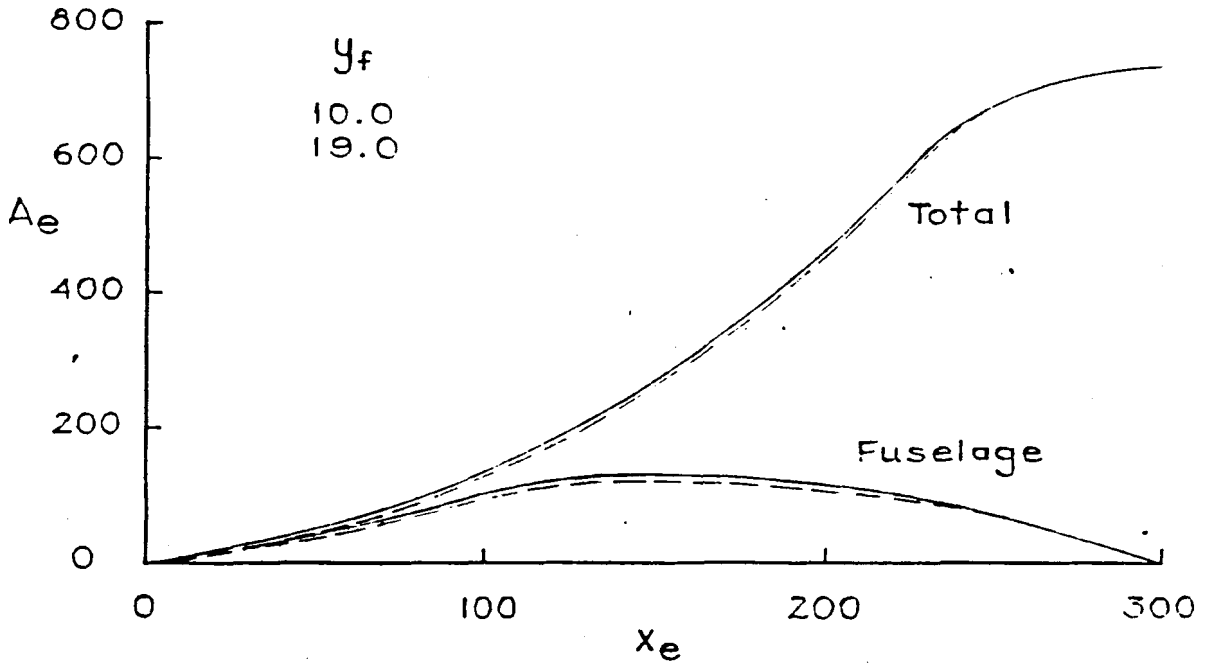

Figure 6. Example of design flexibility possible using the "hybrid" F-function.

In this example, the Mach 1.6 configuration, previously mentioned, serves to demonstrate the increased design flexibility acruing from the use of the "hybrid" F-function derived equivalent area distributions. Its beginning cruise specifications are repeated for ease of referral.

$M = 1.6$,

$h = 45{,}000$ ft,

$W = 650{,}000$ lb,

$l_e = 300.0$ ft,

$\xi = 40.0$ ft, and

$B = 0.5\ \alpha$

A value of about 19.0 feet for y_f will meet "hot day" requirements but results in an aircraft nose that is unusually slender. Decreasing y_f to 10.0 feet while keeping the rest of the input values constant makes the nose blunter and structurally more practical. It also reduces the overpressure. However, this nose shock overpressure reduction will come with the addition of more aircraft volume, and potentially more drag, even though the weight is assumed to have remained constant.

Two pairs of lines are shown in figure 6. The upper pair is for the total equivalent area due to lift and volume, while the lower pair is for the fuselage areas. Reducing yf increases the aircraft volume. This volume increment can be added to the fuselage to permit six-abreast rather than five-abreast seating. If this is not necessary, the extra volume can be used to obtain additional wing volume for fuel. Often, drag and/or weight penalties result from increasing the volume while keeping the length constant. If the drag and weight increments from this volume increase are found to be relatively small, this new low-boom solution may be more suitable than the previous one. The equivalent area curves shown in figure 6 for values of y_f equal to 10.0 and 19.0 feet indicate that over a range of about 220.0 feet in effective length, an increment of about 10.0 square feet in equivalent area would be required.

With the exception of the fuselage, this example is based mostly on overall equivalent areas rather than on actual geometry. If an actual conceptual aircraft were being designed, it is very possible that some of the other parameters would also have to be changed to obtain a good agreement between the aircraft and the ideal equivalent area curves. Obviously, the shape and location of the aircraft components are also changing, but by varying both the aircraft geometry and the low boom equivalent curve, the time required for convergence can be reduced. This double-effort approach assumes that a specified overpressure level is never compromised.

Assuming that the Mach number, the beginning cruise altitude, and the beginning cruise weight are fixed, the values of B and ξ remain as variables to be altered as the design matures. In contrast, the modified Seebass and George F-functions permit changes only in the value of B after fixing the size of y_f and maintaining the other parameters as constants. In the next section, the derivation of the equivalent areas equation is presented and described. The conditions for determining the strength and position of the nose and trailing shocks are also described to show how they are used to determine the necessary constants and coefficients in the area equation.

DERIVATION OF THE "HYBRID" EQUIVALENT AREAS

The F-function shown in figure 4 is inverted by using Abel's integral in the form

$$A_e(x) = 4.0 \int_0^x F(y) \sqrt{x - y}\, dy$$

using the same constraints as in reference 6. It is repeated as figure 7 so the various features can be explained.

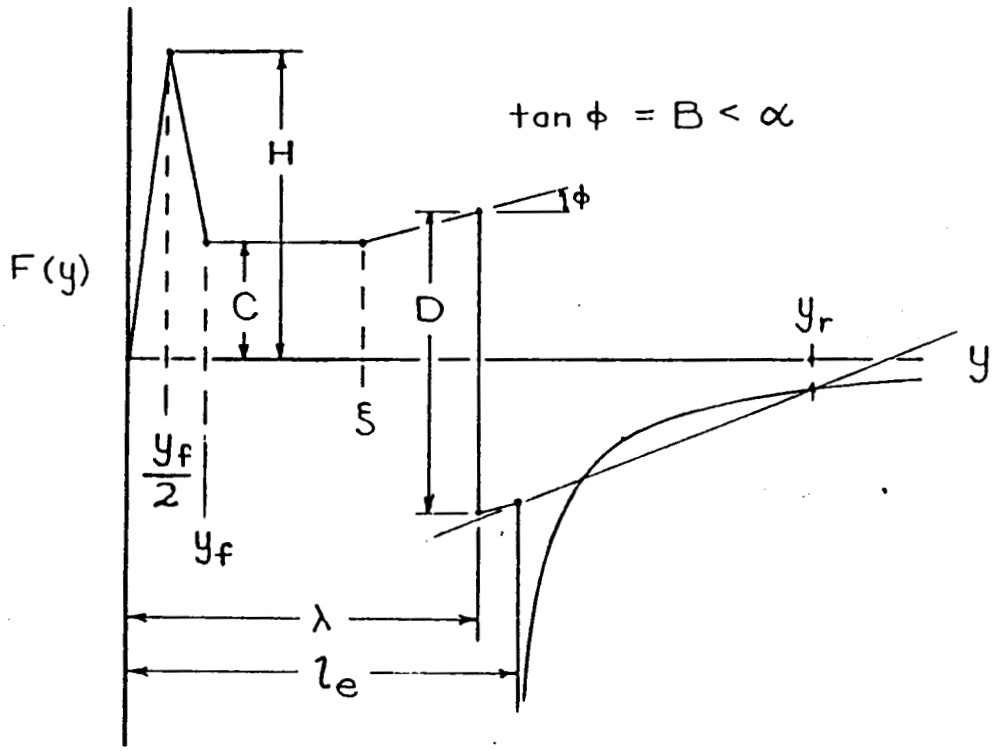

Figure 7. George Haglund's "hybrid" F-function.

The equivalent area associated with this "hybrid" F-function is:

$$A_e(x) = (32/15)\left[(H/y_f)\ x^{5/2} + I(y_f/2)\ \frac{(C-2H)}{y_f}\left(x - \frac{y_f}{2}\right)^{5/2} + I(y_f)\left(\frac{H-C}{y_f}\right)\right.$$

$$\left.(x-y_f)^{5/2} + I(\xi)\,(1/2)\,B\,(x-\xi)^{5/2} - I(\lambda)\,(5/4)\,D\,(x-\lambda)^{3/2}\right]$$

where I(x) is the unit step function.

At $x = l_e$

$$A_e(l_e) = (\beta / 2)\, W/q$$

plus any equivalent area adjustments for wake, boundary layer displacement thickness, engine-nacelle exit area minus intake area increments, etc. Nose shock Δp is computed from the F-function parameter, C, the "advance factor", α, the altitude, h, the reflection factor, K_r, and the ratio of cruise altitude and ground pressures.

As it is applied in this paper

$$\alpha = \Delta F(y)/\Delta y$$

This "advance factor" should not be confused with the "advance" used in the reference 6. There, the advance is called α_x, the distance that a unit disturbance would lead or follow an acoustic signal that reached the ground after propagating through the atmosphere. It would be equal to

$$\alpha_x = C / \alpha$$

The "advance factor" is the change in distance with altitude that a unit strength disturbance travels relative to an acoustic signal starting from the same point along the aircraft during cruise flight. Like the advance, the "advance factor" is calculated from the Mach number, the altitude, and the characteristics of a standard, "hot day", or "cold day" atmosphere. The "advance factor", α, relates the two F-function parameters H and C through

$$H = \frac{C^2}{y_f \alpha} - \frac{C}{2} = \frac{C}{y_f}\alpha_x - \frac{C}{2}$$

The triangular "spike" of magnitude H at $y = y_f/2$ and C at $y = y_f$, is the modification introduced by Darden in reference 7 to reduce the nose bluntness associated with the areas derived from the Dirac-delta function on the F-functions described in reference 6. At $y = \xi$, the constant value of $F(y) = C$, the Haglund innovation, ends, and F(y) continues with slope B past the

discontinuity at $y = \xi$ to $y = l_e$. The value of $\Delta F(y) = D$ at $y = \lambda$, the slope B, and the aircraft or body length l_e are used to set the ratio of tail shock strength to nose shock strength. A solution for the tail shock is found from the value of $F(l_e)$, α, and the integral of F(y) between l_e and an F-function area-balancing point yr which is solved iteratively through

$$0.5\,(F(y_r) - F(l_e))\,(y_r - l_e) = \int_{l_e}^{y_r} F(y)\,dy$$

and

$$\alpha(y_r - l_e) = F(y_r) - F(l_e)$$

Values of y_f, l_e, B, and ξ are part of the input parameter set. Other input parameters include Mach number, altitude, ground reflection factor, and ratio of tail shock strength to nose shock strength. The nose shock strength, Δp, is an output value computed from the input values and shock conditions; it is not a specified or target input. If it is not satisfactory, some of the input lengths, the altitude, the weight, or the Mach number will have to be changed.

The code that computes the hybrid F-function, equivalent areas, and signature is meant to supplement the Seebass and George minimization code. Together, they allow the designer to obtain the possible minimums and then trade sonic boom and atmospheric perturbations with aircraft drag and performance to obtain a satisfactory sonic boom constrained configuration.

CONCLUSIONS

Past experience with sonic boom minimization methods and techniques have shown that the pure mathematical approach has produced two types of performance penalties. The first type was associated with zero-lift wave drag due to the locally severe blunting applied to the nose of the aircraft. This was found with the L.B. Jones lower bound sonic boom body and to a lesser extent, the Seebass and George set of minimum nose shock and minimum overpressure signatures. The second type of penalty was due to the point-design nature of the F-functions or the corresponding pressure signatures. Predicted overpressure signatures might be obtained for a specified standard, hot-day, or cold-day atmosphere, but all three conditions could not be satisfied simultaneously.

A set of empirical cures were found to overcome these limitations. Using a triangular "spike" rather than a Dirac delta-function permitted drag-shock strength trade-offs to be studied

and applied. Combining the "flat-top" and the "ramp" F-function shapes and starting the F-function with the previously-mentioned nose "spike" provided the additional flexibility necessary to meet drag constraints as well as variable atmosphere ambient conditions. The resulting "hybrid" F-function and pressure signature was not a minimum in the mathematical sense, but was a practical compromise in terms of the airplane configuration itself.

Hot day-cold day conditions are small perturbations to the standard day features of the Hybrid F-function. While providing a useful limit on the nose-bluntness length, yf , they should not seriously hamper efforts at setting the "ramp" initial length, ξ , and the "ramp" slope, B, such that aircraft volume, aircraft mission performance, and low sonic boom constraints can be met.

REFERENCES

1. Jones, L. B. : Lower Bounds For Sonic Bangs. Journal of the Royal Aeronautical Society, vol. 65, no. 606, June 1961, pp. 433 - 436.
2. Whitham, G. B. : The Flow Pattern of a Supersonic Projectile. Communication on Pure and Applied Mathematics, vol. V, no. 3, August 1952, pp. 301 - 348.
3. Walkden, F. : The Shock Pattern of a Wing-Body Combination, Far From the Flight Path. Aeronautical Quarterly, vol. IX, pt. 2, May 1958, pp. 164 - 194.
4. McLean, F. Edward : Some Nonasymptotic Effects On the Sonic Boom of Large Airplanes. NASA TN D-2877. 1965.
5. Hayes, Wallace D. ; Haefeli, Rudolph C. ; and Kulsrud, H. E. : Sonic Boom Propagation in a Stratified Atmosphere, With Computer Program. NASA CR - 1299, 1969.
6. Seebass, R. ; and George, A. R. : Sonic-Boom Minimization. Journal of the Acoustical Society of America, vol. 51, no. 2, pt. 3, February 1972, pp. 686 - 694.
7. Darden, Christine M. : Sonic Boom Minimization With Nose-Bluntness Relaxation. NASA TP-1348, 1979.
8. Haglund, George T. : High Speed Civil Transport Design for Reduced Sonic Boom. Boeing Document No. D6-55430, NASA Contract No. NAS1-18377, 1991.